REFERENCES AND NOTES

1. S. Bursztajn, S. A. Berman, W. Gilbert, *Proc. Natl. Acad. Sci. U.S.A.* **86**, 2928 (1989).
2. B. Fontaine and J. P. Changeux, *J. Cell Biol.* **108**, 1025 (1989); O. Horovitz, D. Knaack, T. R. Podleski, M. M. Salpeter, *ibid.*, p. 1823.
3. D. A. Harris, D. L. Falls, G. D. Fischbach, *Nature* **337**, 173 (1989).
4. A. Klarsfeld and J. P. Changeux, *Proc. Natl. Acad. Sci. U.S.A.* **82**, 4558 (1985); A. Klarsfeld, P. Daubas, B. Bourachot, J. P. Changeux, *Mol. Cell. Biol.* **7**, 951 (1987). The AChR α subunit clone used contained 465 nucleotides (nt), consisting of a 340-nt intronic sequence between exons 1 and 2 and a 125-nt portion of exon 2 separated from the intron by a Bgl I sequence. The insert was contained between the Eco RI and Hind III restriction sites of M13mp8. An 80-nt exon probe for AChR was obtained by using Sal I to cut the labeled primer extension product 40 nt into the exon sequence. To obtain an intron probe, we excised a 340-bp Eco RI–Bgl I intron-containing fragment from the clone and cloned it into the Eco RI–Eco RV site of Bluescript KS(−). The single-stranded DNA was synthesized with ^{35}S-labeled deoxyribonucleoside triphosphates (dNTPs) (*1*).
5. Pectoral muscle cells were obtained from 11-day-old chick embryos and plated on collagen-coated cover slips [S. Bursztajn, *J. Neurocytol.* **13**, 501 (1984)]. Cells were maintained in Eagle's minimum essential medium made with Earle's balanced salt solution and supplemented with 10% (v/v) horse serum and embryo extracts. Culture medium was changed every other day, and cells were fixed in 4% paraformaldehyde 4 days after plating. We used a modified hybridization protocol of J. B. Lawrence and R. H. Singer [*Nucleic Acids Res.* **13**, 1777 (1985)]. Cells were washed at room temperature with phosphate-buffered saline (PBS) or stored in 70% ethanol; in the latter case cells were rehydrated for 10 min in PBS containing 5 m*M* $MgCl_2$, followed by a solution containing 0.1*M* glycine and 0.2*M* tris-HCl (*p*H 7.4) for 10 min. Cells were hybridized for 10 min with 50% formamide containing 2× SSC (standard saline citrate) at 65°C (*1*). For each cover slip, 4×10^5 cpm of probe was lyophilized with 40 μg of *Escherichia coli* transfer RNA and 40 μg of sheared salmon sperm DNA, and the mixture was then resuspended in 10 μl of deionized formamide and combined with 10 μl of 4× SSC, 0.4% bovine serum albumin (BSA), 20 m*M* vanadyl ribonucleoside inhibitor, 20% (w/v) dextran sulfate, heparin (1 μg/μl), and 20 m*M* dithiothreitol (DTT). Cells were incubated with the hybridization mixture for 4 hours at 37°C. Cells were then washed at 37°C for 30 min each with 2× SSC containing 50% (v/v) formamide and then 1× SSC containing 50% formamide and finally at room temperature with 1× SSC until almost no radioactivity was detected by a minimonitor. Cover slips were dehydrated through 70%, 95%, and 100% ethanol, attached to slides with Permount, and allowed to dry. Cells were stained with bisbenzimide (Hoechst 33258) and were coated with emulsion (Kodak NTB-3). After 12 days of storage, slides were developed in Kodak D19, and cells were mounted under a cover slip with PBS and glycerol. Cells were observed with a Zeiss microscope equipped with fluorescence optics and a dark-field condenser.
6. J. M. Earley, K. A. Roebuck, W. E. Stumph, *Nucleic Acids Res.* **12**, 7411 (1984). The U1 probe used was derived from 297 bp of the chicken U1 gene cloned into the polycloning site of pUC19. The probe was synthesized with a reverse sequencing primer (New England Biolabs; M13 reverse sequencing primer 1201) and was excised with Eco RI. Synthesis of the probe was performed as for the M13 probe (*1*), except that the template was alkali-denatured in 2*M* NaOH and 2 m*M* EDTA for 5 min at room temperature, and then neutralized while on ice with 3*M* sodium acetate.
7. M. R. Lerner, J. A. Boyle, S. M. Mount, S. L. Wolin, J. A. Steitz, *Nature* **283**, 220 (1980); H. Busch, R. Reddy, L. Rothblum, *Rev. Biochem.* **51**, 617 (1982); I. W. Mattaj, *Trends Biochem. Sci.* **9**, 435 (1984).
8. J. G. Howe and J. Steitz, *Proc. Natl. Acad. Sci. U.S.A.* **83**, 9006 (1986).
9. L. J. Hayward and R. J. Schwartz, *J. Cell Biol.* **102**, 1485 (1986)]; K. S. Chang, N. Rothblum, R. J. Schwartz, *Nucleic Acids Res.* **13**, 1223 (1985). The exon probe used contained 164 bp of exon 7 cloned between the Eco RI and Hind III sites of M13mp19. The actin intron probe was a 290-bp fragment of intron 5 of the actin genomic clone. It was inserted into the Xba I–Hind III site of M13mp18. The single-stranded DNA was synthesized with ^{35}S-labeled dNTPs (*1*).
10. Background counts were determined by counting the number of grains present in areas on cover slips devoid of muscle cells. The average area occupied by 100 nuclei in muscle cells was also determined. The number of background grains per square micrometer of nonmyotube area was determined with the Bioquant morphometry program. This number was then multiplied by the average area of a nucleus to give 0.25 ± 0.10 (mean ± SD) grains per nucleus.
11. N. Hutchison and H. Weintraub, *Cell* **43**, 471 (1985).
12. By fluorescence techniques, J. B. Lawrence, R. H. Singer, and L. M. Marselle [*Cell* **57**, 493 (1989)] detected focal intranuclear localizations of Epstein-Barr virus (EBV) pre-mRNA in EBV-carrying cells in the form of "worm-like" tracks containing several hundred 20-kb RNAs and suggested that these RNAs might be following a transport path.
13. G. Blobel, *Proc. Natl. Acad. Sci. U.S.A.* **82**, 8527 (1985).
14. M. W. Clark and J. Abelson, *J. Cell Biol.* **105**, 1515 (1987).
15. J. P. Merlie and M. M. Smith, *J. Membr. Biol.* **91**, 1 (1986). The Golgi apparatus is circumnuclear in differentiated muscle cells but not in myoblasts or other cells [A. M. Tassin, M. Paintrand, E. G. Berger; M. Borneus, *J. Cell Biol.* **101**, 630 (1985); P. J. Kronebusch and S. J. Singer, *J. Cell Sci.* **1**, 25 (1987); S. C. Miller, G. K. Pavlath, B. T. Blakely, H. M. Blau, *Genes Dev.* **2**, 330 (1988)]. However, transcription, translation, and transport of AChR mRNA are not likely to be simply coupled to the Golgi because the basal amount of AChR mRNA is distributed in the cytoplasm, as revealed with the exon probe (*1*). However, when the amount of AChR mRNA is increased as a result of innervation or external factors, the distribution is predominately perinuclear (*2, 3, 16*).
16. S. A. Berman, S. Bursztajn, W. Gilbert, *Neurosci. Abstr.* **14**, 880 (1988).
17. J. M. Bruner and S. Bursztajn, *Dev. Biol.* **115**, 35 (1986).
18. G. K. Pavlath, K. Rich, S. G. Webster, H. M. Blau, *Nature* **337**, 570 (1989); E. Ralston and Z. W. Hall, *Science* **244**, 1066 (1989).
19. S. Bursztajn *et al.*, *J. Cell Biol.* **101**, 104 (1985).

20. We thank J. P. Changeux and A. Klarsfeld for providing an AChR α subunit clone, R. J. Schwartz for providing a cardiac α actin clone, W. E. Stumph for a U1 RNA clone, and R. L. Erikson and D. P. Richman for helpful comments on the manuscript. Supported in part by NIH grant NS23477 (S.B.). S.A.B. was supported by a Teacher Investigator Development Award (NS00965) and S.B. by a Research Career Development Award (NS00820).

10 August 1989; accepted 17 October 1989

Perceptual Deficits and the Activity of the Color-Opponent and Broad-Band Pathways at Isoluminance

N. K. LOGOTHETIS, P. H. SCHILLER, E. R. CHARLES, A. C. HURLBERT

The deficits in texture, motion, and depth perception incurred in monkeys at isoluminance were compared with the responses of neurons of the color-opponent and broad-band systems in the lateral geniculate nucleus. Texture perception, assumed to be carried by the color-opponent system, and motion and depth perception, ascribed to the broad-band pathway, were all found to be compromised but not abolished at isoluminance. Correspondingly, both the color-opponent and the broad-band systems were affected at isoluminance, but the activity of the neurons in neither system was abolished. These results suggest that impairment of visual capacities at isoluminance cannot be uniquely attributed to either of these systems and that isoluminant stimuli are inappropriate for the psychophysical isolation of these pathways.

INFORMATION IN THE VISUAL SYSTEM, as in sensory systems in general, is processed along several parallel channels. The geniculostriate system of the primate consists of two major pathways with distinct physiological properties, the color-opponent and the broad-band. These pathways remain segregated through several cortical stages and are believed to subserve different visual capacities (*1*). Because cells in the broad-band system do not respond selectively to different wavelengths of light (*2*), it has been thought that this "color-blind" system becomes inactive at isoluminance, leaving only the color-opponent system functional (*3*). On the basis of these ideas, Livingstone and Hubel proposed that those aspects of visual perception compromised at isoluminance (*4*) are mediated by the broad-band system and that such experiments, therefore, could reveal what visual functions are carried by each of these two channels (*5, 6*). To test this hypothesis directly, we set out to compare the perceptual deficits incurred in monkeys at isoluminance with the responses of single cells of the color-opponent and broad-band systems.

We trained rhesus monkeys to detect or discriminate motion, stereoscopic depth, and texture differences in red-green stimuli of various luminance and color contrasts (Fig. 1). Choice of these three visual tasks was based on the assumption that the color-

Department of Brain and Cognitive Sciences, Massachusetts Institute of Technology, Cambridge, MA 02139.

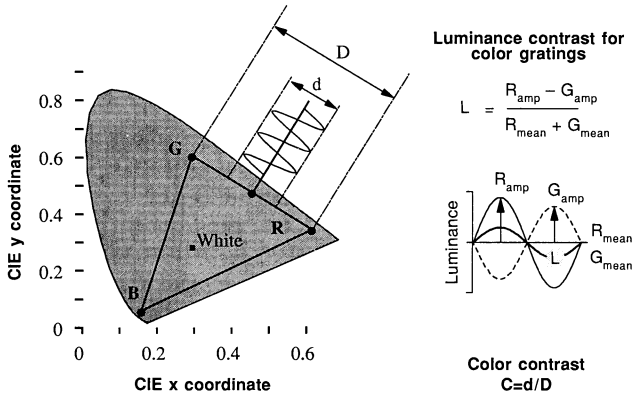

Fig. 1. Color and luminance contrast of the stimuli. The color gratings were generated by adding red (thin solid line) and green (thin dashed line) sinusoidal gratings 180° out of phase. Color contrast (C) was defined as the ratio of the amplitude (d) of the color change along the red-green line of the CIE (Commission Internationale de l'Eclairage) chromaticity diagram to the maximum change possible between the red and green phosphors (D) of our display for a given luminance value represented by the overall size of the color triangle RGB (red, green, blue) (*17*). When the amplitude of the modulation of the red and green were equal as defined with standard psychophysical tests such as flicker photometry, the red-green gratings were isoluminant. Amplitudes of the red and green modulations different from those psychophysically defined as isoluminant resulted in a luminance modulation indicated by the thick solid sinewave. For the color gratings, luminance contrast (L) was expressed as the difference between the two amplitudes of the red and green (R_{amp}, G_{amp}), divided by the mean luminances of the two wave forms (R_{mean}, G_{mean}). For the depth, texture, motion- and flicker-detection tasks, luminance contrast was given as the logarithm of the red and green luminance ratio.

opponent system processes high-resolution static form perception, texture perception being an example, and the broad-band system processes motion perception and stereopsis (*6*). The stimuli were presented on a calibrated and linearized color monitor with a raster display system (*7*). The animals' eye movements were tracked with the scleral-search coil technique (*8*). Data collection, stimulus presentation, and the animals' behaviors were under computer control. The task was to fixate a small spot that appeared at the start of each trial, and then to locate a target that appeared randomly in one of four to eight locations peripheral to the fixation point. The monkey was rewarded for making a single direct saccade to the target. Saccades to other locations aborted the trial.

In the texture-discrimination task, the target was a small square region of diagonal line segments (///) that appeared within a larger array of line segments of the opposite orientation (\\\). In the motion-detection task, the target was a small area of coherently moving dots in a larger array of stationary random dots. For the depth-discrimination task, the monkey stereoscopically viewed Julesz-type (*9*) random-dot stereograms; the target was a small square in depth created by horizontally shifting a square area in one of the stereograms. In both cases the mean luminance of the display varied from 18 to 27 cd per square meter. The isoluminance point of each subject was defined by flicker photometry. Four stimuli, each a 2 × 2 degrees square patch, were presented on the monitor: three were yellow with slight variations in hue and intensity and one was flickered at 15 Hz between red and green. The task was to identify the location of the flickering stimulus, the position of which was randomized by trial. The particular red-green ratio at which discrimination fell to a minimum was the point at which the two colors were of equal luminance (isoluminant) to the subject (*10*).

The performance of one monkey on the texture, motion, and depth tasks is shown in Fig. 2A. We obtained similar results from four other monkeys and from six human subjects tested with the same apparatus. The data show that the perception of texture, motion, and stereoscopic depth was impaired at similar red-green luminance ratios for each task. Performance at zero luminance contrast, however, was significantly better than chance for both motion and stereoscopic tasks. This suggests that color information can, to some extent at least, be used for processing the information required by these tasks.

To examine this question in more detail, we systematically varied color contrast from 0 to 100% for each given luminance contrast, which is shown for one animal for stereopsis in Fig. 2B; as color contrast was reduced, performance fell off. To ascertain that our results were not attributable to axial chromatic aberration of the eye, data for both human subjects and monkeys were collected with blurred stimuli, which, by eliminating sharp borders, minimize these factors (*11*). The data obtained under such conditions also indicate improved performance with increasing color contrast. Thus color cues, although less effective than are luminance cues, can indeed be used for the perception of texture, motion, and stereoscopic depth perception as also suggested by recent psychophysical studies on humans (*12, 13*).

We next examined the responses of single cells in the parvocellular and magnocellular portions of the lateral geniculate nucleus to which the retinal color-opponent and broad-band cells project, respectively. Six animals were used, one of which also served in the behavioral experiments. The stimuli, presented with the same or with a similar system, were spots of various sizes flickering between red and green or moving red-green

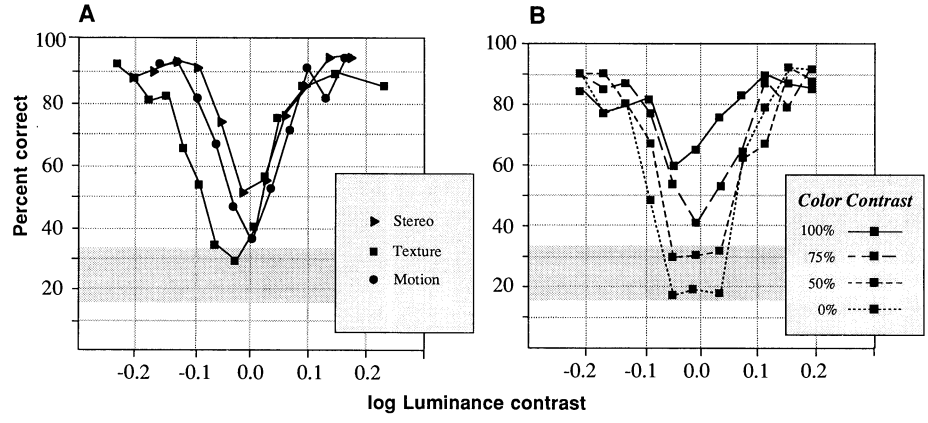

Fig. 2. Stereoscopic depth, texture, and motion perception at isoluminance for one of the tested monkeys. (**A**) Percent correct performance (measured as the percentage of total trials for which the animal correctly located the target) on stereoscopic depth, texture, and motion perception at various luminance contrasts for stimuli of maximum color contrast. The width of the oriented lines in the texture discrimination task was 3.5 minutes of arc; the distance between them was 14 minutes of arc. Targets, presented 2° to 6° eccentric to the fovea, ranged in size from 0.33° to 2° of visual angle. Targets of similar size were used for the detection of stereoscopic depth, with disparities of 3.5 to 12 minutes of arc, and for motion detection, with velocities 6° and 12° per second. Dot size in the random-dot patterns was 12 to 18 minutes of arc diameter. (**B**) Stereoscopic depth perception at various luminance contrasts for four-color contrast values (0, 50, 75, and 100%). Increasing the color contrast improves the performance, as can be seen by comparing the curves. The shaded area in both plots shows the confidence limits for chance performance for significance at the 0.01 level (n = 170; low limit, 16.5%; high limit, 33.5%).

sinusoidal gratings of low spatial frequency. The stimuli were centered on the receptive field of each cell. A range of temporal frequencies and of luminance and color contrasts were examined. For each cell, the luminance of one color was systematically varied within a range of ±0.8 log units around the behaviorally established isoluminance point to determine the contrast that minimized each cell's activity. The responses of two parvocellular cells are shown in the first two columns in Fig. 3. The first became unresponsive at zero luminance contrast. The second cell, which was highly wavelength-selective, continued to respond throughout the contrast range. The third column shows the responses of a typical magnocellular cell. This cell was not silenced at any luminance contrast. At its best balance point (0.2 log units from the isoluminance point), the cell responded equally to both phases of the red-green light exchange. The fourth column shows multiple unit recordings from five to seven magnocellular cells (both ON- and OFF-center cells), demonstrating that the population response did not diminish considerably at or near isoluminance. The distribution of best balance points of all cells studied showed that the red-green zero or balanced contrast varies considerably from cell to cell, particularly for the parvocellular cells (Fig. 4). The variation seen in the magnocellular cells seems adequate to suggest that the system as a whole is not silenced at isoluminance, as directly demonstrated by the multiple unit recording data. These findings are in agreement with earlier studies that used different methods (*14*).

To estimate the extent to which the overall activity of the color-opponent and of broad-band systems declines near isoluminance, we assessed the response of each cell at a red-green ratio of 0.63 (where the mean balance point is for the magnocellular cells) and compared it with responses obtained to the red and green stimuli with a 0.8 log intensity difference between them. For the 66 parvocellular cells, this analysis showed a 3.5-fold mean response decrement; for the 41 magnocellular cells, a 2.6-fold decrement was found. The difference in decrement for the two cell types was not statistically significant ($P = 0.01$).

In conclusion, our psychophysical findings show that texture perception, which is generally believed to be mediated by the color-opponent system, is compromised at isoluminance in a manner similar to motion and stereopsis, which have been proposed to be mediated by the broad-band system (*6*). That color information can to some extent be used for the preparation of motion and stereopsis is supported by the observation that an increase in color contrast improves perceptual performance on these tasks. These findings are in agreement with psychophysical studies (*12*) and with clinical work that shows that patients with major deficits in color discrimination not only have normal chromatic contrast sensitivity but yield normal evoked potentials under isoluminant conditions (*15*). Our physiological data show that, at psychophysically defined isoluminance, both the color-opponent and the broad-band systems continue to respond in the lateral geniculate nucleus but do so at a similarly reduced rate. Taken together, our findings suggest that impairment in vision at isoluminance cannot be attributed uniquely to the inactivation of the broad-band pathway as has been suggested by Livingstone and Hubel (*3, 5, 6*). We propose that the color-opponent system can use both wavelength and luminance information to analyze color and form for object vision (*16*), whereas the broad-band system, although color-blind in the sense that it is probably incapable of discriminating different object colors, can use either wavelength or luminance cues to extract border information for spatial and temporal vision.

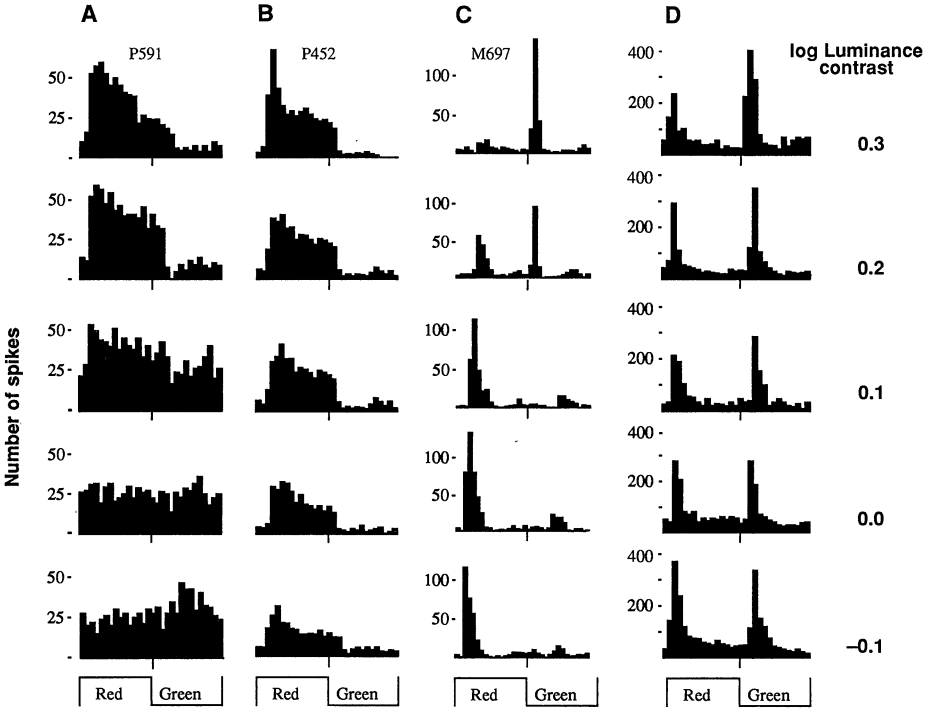

Fig. 3. Single-unit data from the lateral geniculate nucleus. (**A** and **B**) Responses of two parvocellular cells at various luminance contrasts to a flickering red and green light spot of maximum color contrast. Cell P591 became unresponsive at zero luminance contrast; cell P452, which was strongly selective for red, remains active at all contrasts shown. (**C**) The responses of a magnocellular cell for the same stimulation as that used for the cells P591 and P452. The cell is not silenced at any ratio, but exhibits frequency doubling (responds almost equally to both red with green light exchanges) at a contrast of 23%. When the same cell was tested by achromatic stimuli of less than 2.5%, contrast gave no discriminable response. (**D**) Multiple unit responses in magnocellular layers of the lateral geniculate nucleus (five to seven cells, both ON- and OFF-center), showing activity at all red-green luminance ratios. Identical responses were obtained with drifting sinusoidal red-green gratings.

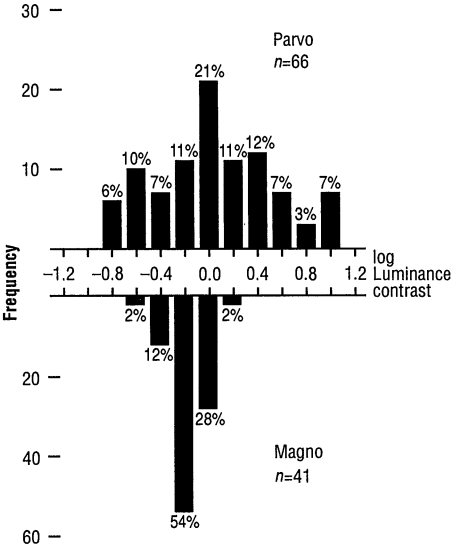

Fig. 4. Histogram showing the distribution of best balance points for parvocellular and magnocellular cells for one of the monkeys. The best balance point is the contrast at which the cell produced balanced responses to both phases of the red-green light exchange for maximum color contrast. For the parvocellular system this point represents the null or zero point, at which the cell gives virtually no response to the red-green alternation. The zero point for parvocellular and the balance point for magnocellular cells both vary from cell to cell, but much more greatly for the former.

REFERENCES AND NOTES

1. E. A. DeYoe and D. C. Van Essen, *Trends Neurosci.* **11**, 219 (1988); P. Lennie, *Vision Res.* **20**, 561 (1980); D. C. Van Essen and J. H. R. Maunsell, *Trends Neurosci.* **63**, 370 (1983); L. G. Ungerleider *et al.*, *J. Comp. Neurol.* **217**, 137 (1983); S. M. Zeki, *Nature* **274**, 423 (1978); ——— and S. Shipp, *ibid.* **335**, 311 (1988).
2. T. P. Hicks *et al.*, *J. Physiol. (London)* **337**, 183 (1983); J. Krueger, *Vision Res.* **19**, 1351 (1979).
3. M. S. Livingstone and D. H. Hubel, *J. Neurosci.* **7**, 3416 (1987).
4. R. L. Gregory, *Perception* **6**, 113 (1977); P. Cavanagh *et al.*, *J. Opt. Soc. Am.* **1**, 893 (1984); C. Lu and D. H. Fender, *Invest Ophthalmol.* **11**, 482 (1972).
5. M. S. Livingstone and D. H. Hubel, *Science* **240**, 740 (1988).
6. M. S. Livingstone, *Sci. Am.* **258**, 78 (January 1988).
7. The stimuli were presented on a Hitachi HM3619A video monitor. The monitor was tested for phosphor and spatial independence, phosphor constancy, and spatial inhomogeneity and was carefully calibrated [D. H. Brainard, *Color Res. Appl.* **14**, 23 (1989)]. To establish a linear relationship between the luminance of the colors and the color entries, we performed a gamma correction [A. B. Watson *et al.*, *Behav. Res. Methods Instrum. Comput.* **18**, 587 (1986)] with software by recalculating the display-data value table. During the intertrial and the fixation period the animal viewed a gray background of 5 cd/m^2 luminance. The mean luminance of the stimuli varied from 5 to 27 cd/m^2. The stimuli used in the neurophysiological experiments were either drifting sinusoidal gratings or flickering spots on a 5 cd/m^2 gray background. The size of the stimuli varied from 0.25° to 4°. The spatial frequency of the sinusoidal gratings varied from 0.1 to 1 cycle per degree. The amplitude of the red modulation of the sinusoidal color gratings was held constant to 14.6 cd/m^2, and the green modulation varied to yield luminance contrast values from 0 to 25%. For the flickering lights the red-green ratio was varied from 1.0 to 10.0 in 0.05 log units.
8. D. A. Robinson, *IEEE Trans. Biomed. Eng.* **101**, 131 (1963).
9. B. Julesz, *Foundations of Cyclopean Perception* (Univ. of Chicago Press, Chicago, 1971).
10. R. L. De Valois, H. C. Morgan, M. C. Polson, W. R. Mead, E. M. Hull, *Vision Res.* **14**, 53 (1974).
11. The major source of luminance contrast artifacts are the axial chromatic aberrations, since lateral chromatic aberrations appear to be corrected by the nervous system [R. Held, in *Visual Coding and Adaptability*, S. Harris, Ed. (Erlbaum, Hillsdale, NJ, 1980), p. 69]. For the display monitor used in these experiments (R = 627 nm, G = 525 nm) when the green color was at zero diopters from the fixation, the red was estimated to be at −0.4 diopters [P. A. Howarth and A. Bradley, *Vision Res.* **26**, 361 (1986)]. For the sinusoidal gratings of the highest used spatial frequency (1 cycle per degree) or for the filtered random dot stereograms, and for a maximum pupil size of 4 mm, the artificial contrast induced by the axial chromatic aberrations at isoluminance was computed to be 1.02%. When we used achromatic stimuli of a contrast less than 2.00%, performance was never improved in the psychophysical experiments and the typical frequency doubling of the magnocellular cells described in this paper was never elicited. We, therefore, believe that the contrast artifacts produced by chromatic aberrations cannot underlie either the effects of color contribution to the perception of motion and stereo or the residual activity of the broad-band system at isoluminance.
12. P. Cavanagh and S. M. Anstis, *Invest. Ophthalmol. Visual Sci. (Suppl.)* **27**, 291 (1986); P. Cavanagh and O. E. Favreau, *Vision Res.* **25**, 1595 (1985); J. P. Comerford, *ibid.* **14**, 975 (1974).
13. C. M. M. de Weert and K. J. Sadza, in *Color Vision: Physiology and Psychophysics*, J. D. Mollon and L. T. Sharpe, Eds. (Academic Press, London, 1983), pp. 553–562.
14. P. H. Schiller and C. L. Colby, *Vision Res.* **23**, 1631 (1983); A. M. Derrington, J. Krauskopf, P. Lennie, *J. Physiol. (London)* **357**, 241 (1984); B. B. Lee, P. R. Martin, A. Valberg, *J. Neurosci.* **9**, 1443 (1989).
15. J. D. Victor, K. Maiese, R. Shapley, J. Sidtis, M. S. Gazzaniga, *Clin. Vision Sci.* **4**, 183 (1989).
16. L. G. Ungerleider and M. Mishkin, in *Analysis of Visual Behavior*, D. J. Ingle, M. A. Goodale, R. J. W. Mansfield, Eds. (MIT Press, Cambridge, 1982), p. 549.
17. P. Cavanagh, C. W. Tyler, O. E. Favreau, *J. Opt. Soc. Am.* **1**, 893 (1984).
18. We thank S. Schein and J. Schall for their comments on the manuscript. Supported by NIH EY00676 to P.H.S.

28 June 1989; accepted 17 November 1989

Target Control of Collateral Extension and Directional Axon Growth in the Mammalian Brain

CHRISTOPHER D. HEFFNER, ANDREW G. S. LUMSDEN, DENNIS D. M. O'LEARY

Individual neurons in the brain send their axons over considerable distances to multiple targets, but the mechanisms governing this process are unresolved. An amenable system for studying axon outgrowth, branching, and target selection is the mammalian corticopontine projection. This major connection develops from parent corticospinal axons that have already grown past the pons, by a delayed interstitial budding of collateral branches that then grow directly into their target, the basilar pons. When cocultured with explants of developing cortex in three-dimensional collagen matrices, the basilar pons elicits the formation and directional growth of cortical axon collaterals across the intervening matrix. This effect appears to be target-specific and selectively influences neurons in the appropriate cortical layer. These in vitro findings provide evidence that the basilar pons becomes innervated by controlling at a distance the budding and directed ingrowth of cortical axon collaterals through the release of a diffusible, chemotropic molecule.

Most regions of the mammalian neocortex send axons to the basilar pons, establishing a major connection that is essential for the control of motor behavior (*1*). The corticopontine projection, which arises from neurons in layer 5 of the neocortex (*2*), develops by a delayed interstitial budding of axon collaterals, rather than through the direct ingrowth of primary axons or of branches formed by bifurcation of their growth cones (*3*). Cortical axons initially grow past the basilar pons and only later do they extend branches into it. This mechanism is used regardless of whether the parent axon's post-pontine segment, which forms the corticospinal projection, is retained (motor cortex) or later eliminated (visual cortex) (*3, 4*). Thus, in this system, unlike others characterized to date (*5*), the target is not recognized by the growth cones of the primary axons. However, the subsequent budding of collaterals at stereotypic positions directly over the basilar pons suggests that cues do identify it as a target of cortical axons.

What mechanism controls the budding and ingrowth of collaterals? One possibility is that collaterals are produced at predetermined points along the axon, or at some predetermined time in its extension according to a program intrinsic to the cortical neuron. Alternatively, the process could be in response to local cues that develop selectively in the region of the corticospinal tract overlying the basilar pons. Another possibility is that the maturing basilar pons induces its own innervation by producing a long-range, chemotropic signal that acts on the overlying cortical axons.

One means of distinguishing among these possibilities is to coculture at a distance explants of cortex and basilar pons within three-dimensional collagen matrices and examine the extent to which cortical axon outgrowth may be stimulated and directed across the intervening collagen matrix. This procedure enables the detection of diffusible, chemotropic activities emanating from target tissue and excludes the action of possible local guidance cues (*6*). Accordingly, explants of postnatal day 0 to 1 rat motor or visual cortex were cultured alone (n = 73) or cocultured (n = 397) in collagen gels with age-matched explants of their normal target tissue, the basilar pons, or a nontarget, control tissue, or both (*7*). Control tissues used were olfactory bulb, hypothalamus, mammillary bodies (tissues at a similar developmental stage as basilar pons, but which do not receive neocortical input),

C. D. Heffner and D. D. M. O'Leary, Department of Anatomy and Neurobiology and Department of Neurology and Neurological Surgery, Washington University School of Medicine, St. Louis, MO 63110.
A. G. S. Lumsden, Department of Anatomy, United Medical and Dental Schools, Guy's Hospital, London, SE1 9RT, England.